Polymer Chemistry

ROYAL SOCIETY OF CHEMISTRY

PAPER

View Article Online
View Journal

Cite this: DOI: 10.1039/d6py00352d

Investigating the solubility of new branched polymers and copolymers synthesised using transfer-dominated branching radical telomerisation (TBRT) of dimethacrylates

Bethany Linthwaite,[a,b] Sean Flynn,[a,b] Oliver B. Penrhyn-Lowe,[a,b] Samuel Mckeating,[a,b] Stephen Wright,[a,b] Savannah R. Cassin,[a,b] Steven L. Brown,[c] Paul H. Findlay,[c,d] Matthew Diable,[a,c,d] Pierre Chambon,[a,b] Andrew B. Dwyer[a,b] and Steve P. Rannard *[a,b]

Transfer-dominated Branching Radical Telomerisation (TBRT) allows the synthesis of high molecular weight branched polymers *via* the homopolymerisation of multi-vinyl substrates without gelation and copolymerisation with mono-vinyl feedstocks. Understanding the key structural and chemical factors influencing the solubility of new polymers may allow careful selection of building blocks when designing specific functions within target environments. Here, a set of 30 (co)polymers were synthesised, creating a diverse library with variation of backbone chemistry, hydrophilicity, polarity, side chain structure, and functionality. Synthesis conditions were varied to enable high molecular weight samples, each closely conforming to ideally branched TBRT structures. Seven solvents with increasing polarity, dipole moment, and dielectric constant were selected to study solubility, as determined after equilibration at ambient temperature. Backbone chemistry and side chain functionality, either delivered *via* telogen or through copolymerisation, was observed to be important. Simplistic rationales relating to solvent parameters were not clearly achievable but the use of contemporary models utilising quantum chemical data and large experimental datasets was remarkably able to predict directional trends in solubility between comparable polymer chemistries through interrogation of repeating units. This offers a computational screening of TBRT (co) polymer designs before undertaking considerable synthesis campaigns.

Received 10th April 2026,
Accepted 18th May 2026

DOI: 10.1039/d6py00352d

rsc.li/polymers

Introduction

The introduction of novel synthetic strategies for homopolymers and copolymers opens new avenues of investigation to researchers around the world. Typically, a new synthesis approach utilises existing monomer chemistries but offers control over various features of the resulting polymers or the conditions under which they may be synthesised. For example, reversible-deactivation radical polymerisations have allowed research teams to synthesise relatively low dispersity polymers with complex architectures without the need for stringent control of reaction conditions that would typically have been employed with 'living' polymerisation techniques.[1,2]

Generally speaking, new polymer syntheses form polymers where many of the physical, thermal, chemical, and mechanical properties are relatively well known. To illustrate this, p(methyl methacrylate), p(MMA), formed by conventional free radical polymerisation of methyl methacrylate monomer would be expected to behave nearly identically to p(MMA) synthesised by atom transfer radical polymerisation or reversible addition–fragmentation chain transfer techniques. This is especially the case when chain lengths are above critical values, such as the point where the glass transition temperature *vs.* molecular weight relationship plateaus as described by Flory–Fox theory.[3]

Despite this, prediction of polymer solubility, especially copolymer solubility, across a range of solvents and with unusual monomer compositions is non-trivial. This is important in many fields including understanding phase transitions, predicting compatibility with new solvents, and formulating products containing reactive diluents.[4] Predicting the solubi-

[a]*Department of Chemistry, University of Liverpool, Crown Street, L69 7ZD, UK. E-mail: srannard@liv.ac.uk*
[b]*Materials Innovation Factory, University of Liverpool, Crown Street, L69 7ZD, UK*
[c]*Scott Bader Ltd, Wollaston Hall, Wollaston, Wellingborough, Northamptonshire, NN29 7FH, UK*
[d]*Polymer Mimetics Ltd, Innovation Centre One, 131 Mount Pleasant, Mount Pleasant, Liverpool Science Park, Liverpool, L3 5TF England, UK*

lity of small molecules is challenging in itself,[5] but the additional complexity that is derived from molecular weight distributions, compositional diversity within copolymer samples, architecture variation, and unknown or unmeasured polymer–solvent interaction parameters present considerable additional hurdles for accurate prediction of solubility or trends that may be expected across a targeted range of polymers.[6]

In summary, the approaches to polymer solubility prediction can be categorised as: (1) theoretical models;[7] (2) computation and simulation;[7–9] (3) machine learning algorithms;[10] (4) experimental approaches (including library synthesis);[11] and (5) hybrid techniques such as high-throughput screening combined with machine learning.[12] Concepts such as Hansen or Hildebrand solubility parameters and Flory–Huggins interaction parameters are based on the concept of "like-dissolves-like" and are relied upon by many in industrial settings.[12,13] With entirely new (co)polymers or new solvents, some parameters need to be estimated due to the lack of background data. Machine learning approaches may also suffer from a dearth of experimental data to draw upon, or variable quality data generated using inconsistent methodologies.[4,14,15] Experimental approaches aiming to synthesise large libraries of new macromolecules and screen solubility across wide solvent ranges are also resource intensive.

In recent years, the introduction of transfer-dominated branching radical telomerisation (TBRT) as a new synthesis approach has been shown to provide entirely novel branched homopolymers and copolymers.[16–19] Despite predominantly using commercial feedstocks, these branched macromolecules have not previously been available for study as conventional polymerisation techniques would result in insoluble crosslinked network formation. The mechanism of TBRT allows homopolymerisation of multi-vinyl building blocks, and copolymerisation with low concentrations of mono-vinyl monomers, leading to soluble branched architectures with backbone repeating chemistries that resemble step-growth structures despite the use of conventional free radical chemistry.[20,21] The synthesis of branched polymers and copolymers by TBRT is summarised in Fig. 1A. Importantly, vinyl feedstocks for telomerisation reactions are known as *taxogens*, and chain-transfer agents, are known as *telogens*.[22] By maintaining a number-average chain length derived from vinyl group propagation at <2 units, gelation is avoided with complete consumption of vinyl functionality.[16,21] This typically requires an excess of telogen to generate reaction conditions where telogen-telogen radical chain transfer dominates and propagation is considerably curtailed. The formation of structural subunits with a degree of polymerisation of just one unit, DP_1, is critical to success.[16,23]

Multi-vinyl taxogens (MVTs) may be homopolymerised by TBRT with selection of MVT structure dictating the backbone of the resulting branched polymer, Fig. 1Bi. Mono-VTs may also be included into the reaction mixture and generate branched copolymers, Fig. 1Bii.[17,19] To simplify visualisation of these complex macromolecules, they may be summarised as nominal repeating structures, especially as, under ideal conditions, the telogen is incorporated at a 1 : 1 molar ratio with MVT; if a 1 : 1 : 1 molar ratio of MVT : mono-VT : telogen is targeted, a relatively simple copolymer nominal repeat unit may also be drawn that includes all feedstocks, Fig. 1B.[20]

The consequence of a 1 : 1 molar ratio of MVT : telogen in the final polymer is that the telogen may be considered as a side chain (pendant group) to the backbone. Equally, at a 1 : 1 : 1 molar ratio of MVT : mono-VT : telogen the mono-VT acts to introduce additional side chain functionality.[17] Modification of telogen chemistry, mono-VT, and MVT have all been shown to impact the thermal properties of TBRT polymers and copolymers.[17,24] Here we aimed to investigate the impact of such changes on the solubility of a systematically changing series of TBRT polymers and copolymers.

Synthesis and characterisation of homo- and statistical copolymers by TBRT

To investigate the impact of TBRT polymer backbone structure on experimental solubility, a diversity of starting materials was selected that offers significant backbone variation with respect to hydrophilicity, polarity, aromaticity and rigidity. The MVTs chosen were glycerol dimethacrylate (GDMA) and bisphenol A dimethacrylate (BPADMA), Fig. 1Ci & Cii respectively. For clarity, GDMA is known to be a mixture of 1,2- and 1,3-isomers.[25] To establish the impact of additional functional and non-functional side chains within copolymers, four mono-VTs were selected, namely: isobornyl methacrylate (IBOMA, Fig. 1Di); glycidyl methacrylate (GlyMA, Fig. 1Dii); 2-*N*-morpholinoethyl methacrylate (MEMA, Fig. 1Diii), and glycerol methacrylate (GMA, Fig. 1Div), offering a range of steric crowding, polarity, and hydrophilicity. The telogen structure presents side chains in homopolymer structures and three telogens that introduce diverse chemistries with previously reported success in TBRT were chosen, these were 1-thioglycerol (TG, Fig. 1Ei), *t*-butyl benzyl mercaptan (*t*BuBzM, Fig. 1Eii), and 1-dodecanthiol (DDT, Fig. 1Eiii). Collectively, these nine starting materials, when targeting 1 : 1 : 1 statistical copolymers offer a library of thirty materials, Table 1.

The samples were analysed using Triple-Detection Size Exclusion Chromatography (TD-SEC) to establish comparable values of molecular weight and related properties without resorting to linear polymer standards (Fig. S1). Targeting of molecular weight with TBRT is not trivial and currently requires empirical determination of the relationship with respect to MVT : Telogen ratios.[24] As with many TBRT batch reactions, a telogen excess is required to prevent gelation and as the MVT : Telogen ratio increases, weight-average molecular weight, M_w, values increase dramatically leading eventually to gelation. Number-average molecular weight, M_n, may remain relatively low as a consequence of the intermolecular branching reaction proceeding *via* mechanisms analogous to step-growth curing reactions. Accurate values of $[MVT]_0 : [mono\text{-}VT]_0 : [Tel]_0$ ratios were determined by ^1H nuclear magnetic resonance spectroscopy (NMR) of reaction mixtures prior to thermal initiation (Fig. S2).

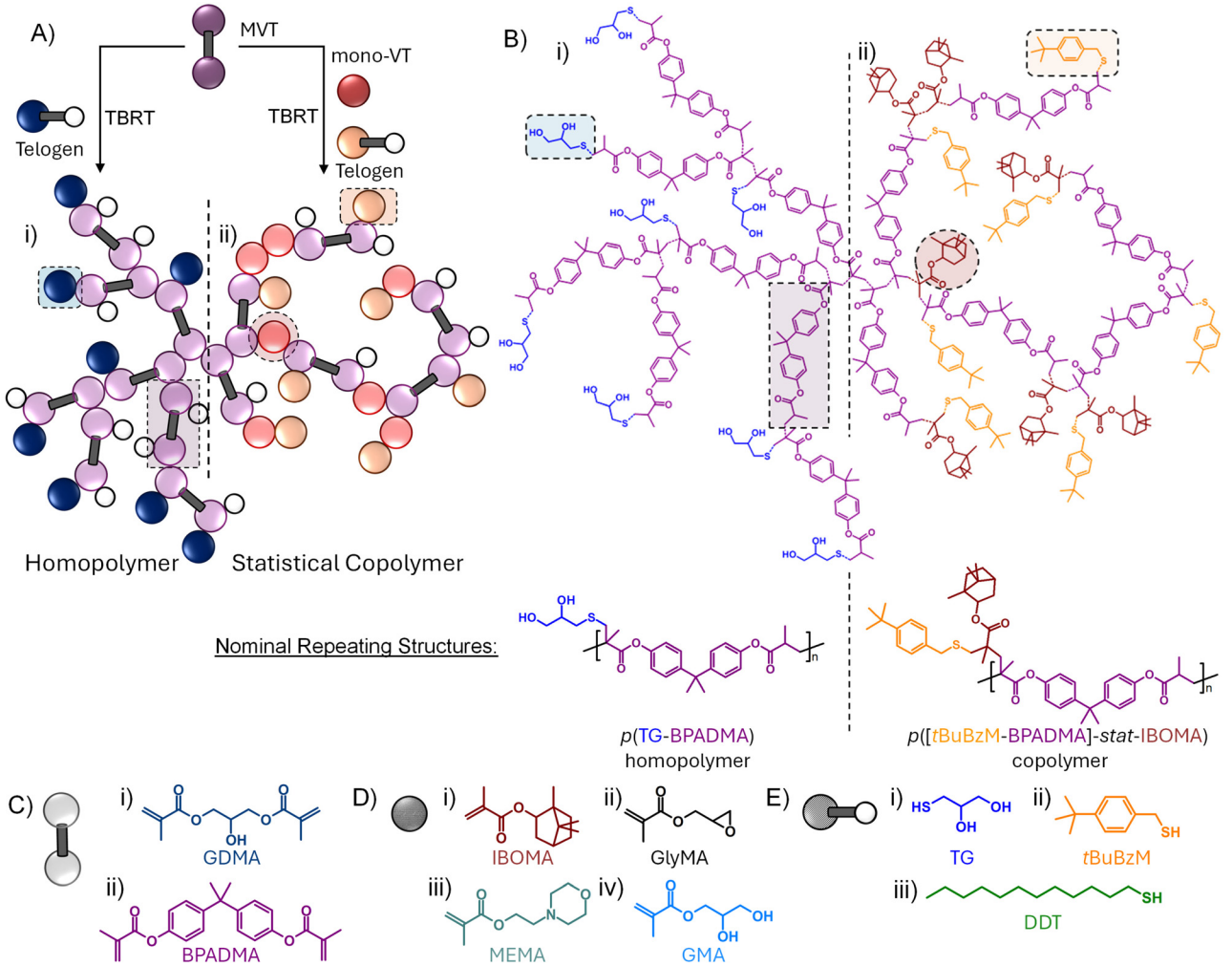

Fig. 1 Schematic representation of branched homopolymers and statistical copolymers synthesised using TBRT. (Ai) homopolymer formed from TBRT reaction of one multi-vinyl taxogen (MVT) and one telogen, and (Aii) statistical copolymer formed using a telogen and a mixed MVT/mono-vinyl taxogen (mono-VT) feedstock; (Bi) structure of TBRT homopolymer formed from 1-thioglycerol (TG) and bisphenol A dimethacrylate (BPADMA) with nominal repeating unit structure, and (Bii) structure of TBRT statistical copolymer synthesised using *t*-butyl benzyl mercaptan (*t*BuBzM) and a mixed feedstock of BPADMA and isobornyl methacrylate (IBOMA); (C) structures of MVTs chosen for the study: (i) glycerol dimethacrylate (GDMA); and (ii) BPADMA; (D) structures of mono-VTs selected for this study: (i) IBOMA; (ii) glycidyl methacrylate (GlyMA); (iii) 2-*N*-morpholinoethyl methacrylate (MEMA); and (iv) glycerol methacrylate (GMA); (E) selected study telogens: (i) TG; (ii) *t*BuBzM; and 1-dodecanthiol (DDT).

Of the thirty homopolymers/copolymers synthesised here, only two have been previously reported: namely the homopolymers p(DDT-BPADMA) and p(*t*BuBzM-BPADMA).[17] Appreciable M_n and M_w were sought for each sample composition to avoid solubility studies being affected by low molecular weight fractions. It is the case that a range of M_n values are present within this study set despite M_w values being very high in some cases. A significant study of each of the targeted compositions was conducted to generate appropriate MVT : Telogen and MVT : mono-VT : Telogen ratios to obtain high M_w samples of each polymer and statistical copolymer. This entailed >120 polymerisation reactions to select the thirty samples studied here. TBRT reactions may be manipulated by reaction concentration, solvent, and temperature and considerable variation was used to obtain the sample library (Table S1).

Rigorous purification of each sample was conducted, including multiple precipitations, to ensure the removal of unreacted telogen that may influence solubility measurements. Again, significant investigation was required to establish appropriate anti-solvents for each sample, especially given the expected impact on solubility that was targeted within their compositions (Table S1). As such, the M_n values shown for some samples are uncharacteristically high for TBRT polymers. For example, p([TG-GDMA]-*stat*-MEMA) required significant precipitation and reprecipitation steps to remove unreacted 1-thioglycerol, and fractionation of the lowest molecular weight species may be the cause of the measured M_n = 45 070 g mol^{-1}. M_n values cannot be directly dictated using TBRT at this stage.

All but one of the final purified polymer or statistical copolymer samples had M_w values > 50 000 g mol^{-1}, and twenty-

Table 1 Characterisation of TBRT homopolymers and statistical homopolymers synthesised during this study. Reactions conducted under a variety of conditions (Table S1) and vinyl group consumption calculated as >99% for all reactions *via* NMR analysis of crude reaction mixtures

	Reaction and recovered (co)polymer composition		TD-SEC				
Polymer	$[MVT]_0$: $[mono\text{-}VT]_0$: $[Tel]_0$	$[MVT]_F$: $[mono\text{-}VT]_F$: $[Tel]_F$ [c]	M_w (g mol^{-1})	M_n (g mol^{-1})	$Đ$	MHSα	dn/dc
Homopolymers							
p(DDT-GDMA)	0.58 : 1 [a]	1.04 : 1 [a]	665 700 [e]	30 370	21.9	0.25	0.106
p(*t*BuBzM-GDMA)	0.77 : 1 [a]	0.99 : 1 [a]	488 800 [e]	3560	137.3	0.29	0.140
p(TG-GDMA)	0.22 : 1 [a]	1.04 : 1 [a]	101 900 [e]	3130	32.6	0.32	0.133
p(DDT-BPADMA)	0.35 : 1 [a]	0.92 : 1 [a]	561 500 [f]	5470	102.7	0.32	0.140
p(*t*BuBzM-BPADMA)	0.44 : 1 [a]	1.01 : 1 [a]	314 600 [f]	13 500	23.3	0.45	0.169
p(TG-BPADMA)	0.25 : 1 [a]	1.04 : 1 [a]	901 710 [e]	14 680	61.4	0.38	0.195
Statistical copolymers							
p([DDT-GDMA]-*stat*-GMA)	0.61 : 0.66 : 1 [a]	*	788 400 [e]	12 110	65.1	0.33	0.108
p([*t*BuBzM-GDMA]-*stat*-GMA)	0.62 : 0.59 : 1 [a]	0.96 : 0.95 : 1 [d]	81 300 [e]	18 290	4.4	0.31	0.132
p([TG-GDMA]-*stat*-GMA)	0.43 : 0.41 : 1 [b]	*	142 200 [e]	2980	47.7	0.29	0.112
p([DDT-GDMA]-*stat*-GlyMA)	0.45 : 0.43 : 1 [a]	1.08 : 1.03 : 1 [a]	99 800 [e]	8920	11.2	0.25	0.120
p([*t*BuBzM-GDMA]-*stat*-GlyMA)	0.34 : 0.35 : 1 [a]	1.02 : 0.87 : 1 [d]	76 700 [e]	4340	17.7	0.29	0.150
p([TG-GDMA]-*stat*-GlyMA)	0.44 : 0.46 : 1 [a]	*	585 400 [e]	3850	152.1	0.34	0.088
p([DDT-GDMA]-*stat*-IBOMA)	0.62 : 0.59 : 1 [a]	*	46 900 [f]	6730	7.0	0.28	0.100
p([*t*BuBzM-GDMA]-*stat*-IBOMA)	0.69 : 0.75 : 1 [a]	0.97 : 0.98 : 1 [a]	105 700 [e]	18 660	5.7	0.27	0.093
p([TG-GDMA]-*stat*-IBOMA)	0.54 : 0.55 : 1 [a]	*	106 400 [e]	3650	29.2	0.28	0.126
p([DDT-GDMA]-*stat*-MEMA)	0.66 : 0.71 : 1 [a]	1.03 : 1.07 : 1 [d]	609 600 [e]	24 960	24.4	0.35	0.096
p([*t*BuBzM-GDMA]-*stat*-MEMA)	0.68 : 0.68 : 1 [a]	1.09 : 1.10 : 1 [d]	131 600 [e]	13 680	9.6	0.29	0.125
p([TG-GDMA]-*stat*-MEMA)	0.56 : 0.56 : 1 [b]	1.02 : 0.98 : 1 [d]	988 800 [e]	45 070	21.9	0.42	0.118
p([DDT-BPADMA]-*stat*-GMA)	0.33 : 0.35 : 1 [a]	1.04 : 1.06 : 1 [a]	1 312 600 [e]	11 460	114.5	0.34	0.129
p([*t*BuBzM-BPADMA]-*stat*-GMA)	0.33 : 0.37 : 1 [b]	*	141 700 [e]	7800	18.2	0.25	0.172
p([TG-BPADMA]-*stat*-GMA)	0.15 : 0.17 : 1 [b]	*	161 164 [e]	4610	34.9	0.31	0.177
p([DDT-BPADMA]-*stat*-GlyMA)	0.30 : 0.30 : 1 [a]	0.86 : 0.53 : 1 [a]	47 200 [f]	7260	6.5	0.31	0.131
p([*t*BuBzM-BPADMA]-*stat*-GlyMA)	0.41 : 0.41 : 1 [a]	1.07 : 0.56 : 1 [a]	367 100 [e]	13 790	26.6	0.34	0.151
p([TG-BPADMA]-*stat*-GlyMA)	0.13 : 0.13 : 1 [a]	*	50 400 [e]	3670	13.7	0.28	0.169
p([DDT-BPADMA]-*stat*-IBOMA)	0.39 : 0.39 : 1 [a]	0.96 : 0.73 : 1 [a]	143 400 [f]	9100	15.8	0.36	0.124
p([*t*BuBzM-BPADMA]-*stat*-IBOMA)	0.44 : 0.46 : 1 [a]	0.93 : 0.68 : 1 [a]	302 100 [f]	7600	39.8	0.40	0.148
p([TG-BPADMA]-*stat*-IBOMA)	0.37 : 0.36 : 1 [a]	0.98 : 0.40 : 1 [a]	152 800 [e]	15 270	10.0	0.30	0.171
p([DDT-BPADMA]-*stat*-MEMA)	0.40 : 0.40 : 1 [a]	0.91 : 0.59 : 1 [a]	124 800 [f]	14 820	8.4	0.37	0.136
p([*t*BuBzM-BPADMA]-*stat*-MEMA)	0.42 : 0.43 : 1 [a]	0.91 : 0.53 : 1 [a]	221 100	10 270	21.5	0.40	0.152
p([TG-BPADMA]-*stat*-MEMA)	0.18 : 0.18 : 1 [a]	1.09 : 0.67 : 1 [a]	279 800 [e]	19 750	14.2	0.33	0.160

*Analysis not possible due to overlapping resonances. [a] Determined by ^{1}H NMR ($CDCl_3$ or d_6-DMSO) from the reaction mixture (t = 0). [b] Determined using exact mass added to reaction mixture. [c] Determined by ^{1}H NMR ($CDCl_3$ or d_6-DMSO) for a sample after purification and drying *in vacuo*. [d] Determined by inverse-gated ^{13}C NMR ($CDCl_3$ or d_6-DMSO). [e] Determined by TD-SEC using DMF eluent system. [f] Determined by TD-SEC using 2% v/v TEA/THF eluent system.

eight samples were characterised with M_n values >3500 g mol^{-1}. As the solubilities of TBRT branched polyesters has not been studied previously, these criteria were considered to be appropriate for this investigation. Also worthy of note is the difficulty encountered when incorporating GlyMA into statistical copolymers with BPADMA. When using TG or DDT as telogens the conventional systematic variation of MVT : Telogen ratios led to gelation at relatively low MVT : Telogen ratios and did not provide the steady rise in M_w that we typically have reported. We therefore targeted relatively low values for p([DDT-BPADMA]-*stat*-GlyMA) and p([TG-BPADMA]-*stat*-GlyMA). This may be an unwanted side reaction with the epoxide ring, but no such issues were observed when employing *t*BuBzM as the telogen, Table 1.

For all samples, the Mark–Houwink–Sakurada (MHS) alpha values were <0.45 and consistent with compact, branched architectures. As would be expected for an ideal TBRT with minimal cyclisation, the MVT : Telogen ratios within the final purified polymers adhered closely to the expected 1 : 1 value.[26,27] Accurate determination of these values was predominantly achieved using ^{1}H NMR (Fig. S3), however, where this was not possible due to overlapping resonances, inverse-gated ^{13}C NMR was required (Fig. S4).[28] For eight of the samples, accurate determination of final composition was not possible using NMR techniques due to a lack of clearly defined resonances that could be accurately utilised. As stated above, the targeted (co)polymers were designed to show a significant variation in solubility, and this was indeed seen during analysis, with several of the samples requiring TD-SEC analysis using DMF eluent although THF was more appropriate for others.

TBRT homo- and statistical copolymer solubility studies

To evaluate the solubility trends within the TBRT polymer/statistical copolymer library, a series of seven solvents were

Table 2 Characteristics of solvents selected for solubility studies

Solvent	Polarity index	Dipole moment (D)	Dielectric constant	Eluotropic strength[a] (ε°)
Water	10.2	2.90[b]	80.1	0.95
Methanol	5.1	2.87	32.7	0.95
Acetone	5.1	2.69	20.7	0.56
Tetrahydrofuran	4.0	1.75	7.58	0.45
Diethyl ether	2.8	1.15	4.33	0.38
Xylene	2.5	0.45	2.57	0.26
Hexane	0.1	0.08	1.88	0.01

[a] Values for Al_2O_3 stationary phase. [b] Value of condensed water.[36]

selected with decreasing polarity, Table 2.[29] Empirical polarity scales for different organic solvents have been relied upon for many years to aid the understanding of solvation and organic solvent behaviour, although recent reports have questioned the underlying principles of established techniques for determining such values.[30] Other values may also be used to characterise different solvents, such as their dipole moment, dielectric constant and eluotropic strength,[31] more commonly used in chromatographic considerations of solvent choice. Across all of these measures, the seven selected solvents showed a broad diversity of values that decreased systematically from water to hexane, Table 2. Importantly, despite the solubility of many compounds being reported on a nominal scale ranging from "insoluble" to "highly soluble" the definitions of terms like "partially soluble" or "freely soluble" are either very broad or not adhered to consistently. Such terms are more common in the drug discovery field,[32,33] however, we have chosen to adopt a similar approach to compartmentalise our results here. With this in mind, our solubility studies accurately weighed approximately 100 mg of each polymer into vials and 1 mL of each solvent was added (for clarity, sample masses were all measured but 100 mg was sometimes difficult to achieve exactly due to the varying physical nature of the polymer samples). The samples were kept at ambient temperature for two weeks, filtered and the mass of polymer within the solvent phase was determined gravimetrically as a mg mL^{-1} value. The long equilibration time was selected to overcome slow dissolution kinetics that would result from variation in glass transition temperature and limited solvent diffusion, and the variability in molecular weight and dispersity within this study set.[34,35]

Significant entanglement is not expected to impact these studies due to the branched architectures within TBRT samples.[37] Polymers with measured solubility values in the range 0–5 mg mL^{-1} were deemed "poorly soluble" whilst samples showing solubilities from 5–20 mg mL^{-1} were considered "slightly soluble". Values of 20–50 mg mL^{-1} were categorised as "soluble" and polymers exhibiting solubilities >50 mg mL^{-1} were considered "highly soluble". This nomenclature is purely employed to aid the differentiation of solubility behaviour of these materials, and all measured values are also presented (Table S2).

TBRT polymers are novel branched polyesters with several structural variables. As homopolymers, their behaviour has been shown to be dictated by both the backbone, derived from the MVT, and the telogen, acting as side chain.[17] Within their architecture there are three structural sub-units that mirror the components of conventional AB_n hyperbranched polymers.[38] *Terminal* groups are derived from the simple addition of the telogen to one vinyl group of the MVT with no propagation, *i.e.* a DP_1 sub-unit. These dominate the structure and may be critical in determining solubility characteristics through polymer-solvent and polymer–polymer interactions. *Linear* sub-units are formed when the propagation is limited to DP_2 and do not contribute to branching. Any propagation >2 vinyl units will lead to branching and become *dendritic* sub-units, and these vary in length and position within the architecture, Fig. 1Ai & Bi.[28]

TBRT copolymers derived from mono-VT incorporation offer additional complexity. Not only do they add additional side chains to the branched architecture, they may carry functional groups and impact inter- and intra-chain interactions. When incorporated into a terminal sub-unit they modify the chemistry of the surrounding environment but do not increase branching. When adding into linear and dendritic sub-units and, the overall DP_n increases and a new chemical environment is created but, again, no change in branching occurs as the mono-VT increases the length of the sub-unit but not its multiplicity. The process of mono-VT incorporation is statistical so different terminal units will now be present, including those with no mono-VT, those with one mono-VT and, potentially, multiple monofunctional comonomers added. Additionally, within the linear and dendritic sub-units, single mono-VT residues may be isolated within telomer chains formed only from MVT propagation or multiple mono-VTs may be present and may be incorporated next to each other, Fig. 1Aii & Bii.[17]

The complexity of TBRT statistical copolymers is not entirely dissimilar to the that seen is conventional linear statistical co- and terpolymers but somewhat enhanced by the architectural variation.[39,40] Due to the statistical nature of these polymers, broad molecular weight distributions also complicate any overall prediction of solubility behaviour.

Effects of telogen and mono-VT on solubility behaviour

It was immediately apparent that the different structural components of TBRT homo- and copolymers were able to exert a significant impact on their solubility. As an exemplar selection of the data derived during this study, fifteen polymers are shown with their measured solubility in water, methanol and hexane in Fig. 2.

When considering the GDMA-derived backbone polymers, the impact of telogen chemistry is apparent within the homopolymer, **1–3**, solubility in water and methanol, Fig. 2A. Despite the presence of a pendant hydroxyl functional group within the MVT, p(DDT-GDMA), **1**, and p(*t*BuBzM-GDMA), **2**,

are essentially insoluble in water, however, substitution of the telogen within these structures to TG creates a slightly soluble homopolymer (p(TG-GDMA), **3**, [water] = 9.1 mg mL^{-1}). This same effect, although more dramatic, is seen across dissolution in methanol, with p(DDT-GDMA), **1**, remaining poorly soluble, p(*t*BuBzM-GDMA), **2**, determined as soluble, and p(TG-GDMA), **3**, being highly soluble, Fig. 2A. Interestingly, these three homopolymers show poor solubility in hexane suggesting the MVT is dominating solubility behaviour in this case, and telogen chemistry alone is not able to overcome the need to solvate the backbone in order to form solutions of appreciable concentration.

Mono-VTs have been shown to modify thermal properties of TBRT copolymers. The introduction of GMA would be expected to increase the hydrophilicity of the TBRT copolymers, **4–6**, relative to their respective homopolymers. From a perspective of water solubility, this is not specifically seen for p([DDT-GDMA]-*stat*-GMA), **4**, and p([*t*BuBzM-GDMA]-*stat*-GMA), **5**, with both materials remaining poorly soluble.

A significant improvement in water solubility was observed when 1-thioglycerol is present as the telogen with p([TG-GDMA]-*stat*-GMA), **6**, measured as having a solubility within our defined "soluble" range ([water] = 25.2 mg mL^{-1}) and considerably higher than the p(TG-GDMA) homopolymer, Fig. 2A.

The three GMA-containing copolymers, **4–6**, were readily determined to be "highly soluble" in methanol. The impact of GMA on methanol solubility was particularly notable when comparing p(DDT-GDMA) (**1**, [methanol] = <1.0 mg mL^{-1}) and p([DDT-GDMA]-*stat*-GMA) (**4**, [methanol] = 90.1 mg mL^{-1}), Fig. 2A. Again, no meaningful solubility in hexane was observed across these GMA-containing copolymers.

The analogous copolymers p([DDT-GDMA]-*stat*-IBOMA), **7**, p([*t*BuBzM-GDMA]-*stat*-IBOMA), **8**, and p([TG-GDMA]-*stat*-IBOMA), **9**, showed no appreciable water solubility with the presence of the highly hydrophobic and bulky IBOMA side chain preventing solvation of the hydrophilic backbone. Relative to the homopolymers, solubility in methanol was increased for p([DDT-GDMA]-*stat*-IBOMA), **7**, into the "slightly soluble" range, and decreased for p([*t*BuBzM-GDMA]-*stat*-IBOMA), **8**, from the borderline of "slightly soluble"/"soluble" to the border of "poorly soluble". The high solubility of p([TG-GDMA]-*stat*-IBOMA) copolymer, **9**, in methanol ([methanol] = 84.7 mg mL^{-1}) mirrored the homopolymer p(TG-GDMA), **3**, and p([TG-GDMA]-*stat*-GMA), **6**. From a purely structural point of view, p([TG-GDMA]-*stat*-IBOMA), **9**, p([DDT-GDMA]-*stat*-GMA), **4**, and p([*t*BuBzM-GDMA]-*stat*-GMA), **5**, all display a hydrophilic diol and a hydrophobic side chain but derived from different species, namely telogen and mono-VT (**9**) or mono-VT and telogen (**4** and **5**) respectively. The similarity in their methanol solubilities can, therefore, be rationalised using the same principles. The solubility of IBOMA-containing copolymers in hexane also mirrors the pre-

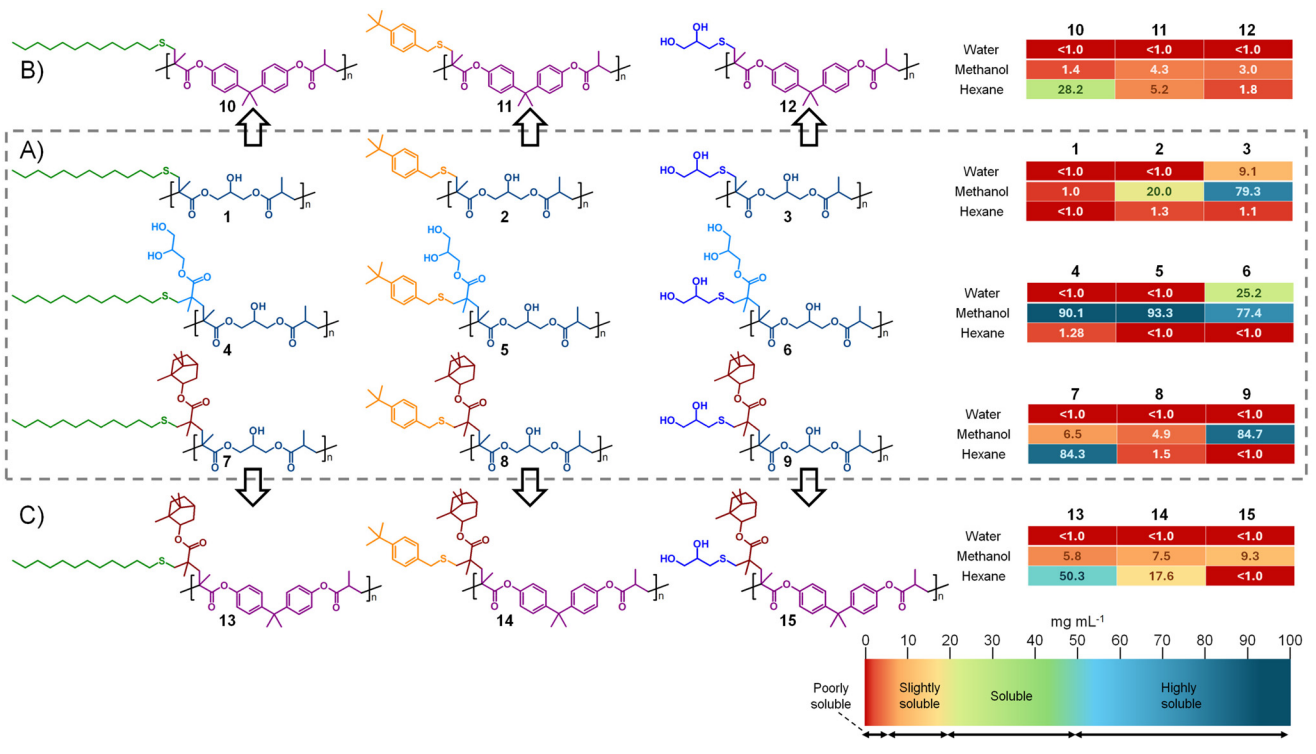

Fig. 2 Initial solubility evaluation of comparative samples of homopolymers and statistical copolymers synthesised by TBRT in water, methanol and hexane (values in mg mL^{-1}): (A) homopolymer p(DDT-GDMA) **1**; homopolymer p(*t*BuBzM-GDMA) **2**; homopolymer p(TG-GDMA) **3**; p([DDT-GDMA]-*stat*-GMA) **4**; p([*t*BuBzM-GDMA]-*stat*-GMA) **5**; p([TG-GDMA]-*stat*-GMA) **6**; p([DDT-GDMA]-*stat*-IBOMA) **7**; p([*t*BuBzM-GDMA]-*stat*-IBOMA) **8**; and p([TG-GDMA]-*stat*-IBOMA) **9**. (B) homopolymer p(DDT-BPADMA) **10**; homopolymer p(*t*BuBzM-BPADMA) **11**; and homopolymer p(TG-BPADMA) **12**. (C) p([DDT-BPADMA]-*stat*-IBOMA) **13**; p([*t*BuBzM-BPADMA]-*stat*-IBOMA) **14**; and p([TG-BPADMA]-*stat*-IBOMA) **15**.

vious homopolymers and copolymers containing GMA, with the exception of p([DDT-GDMA]-*stat*-IBOMA), **7**. The combination of DDT and IBOMA side chains within **7** clearly overcomes the GDMA-derived backbone chemistry to allow a "highly soluble" copolymer to be formed ([hexane] = 84.3 mg mL^{-1}).

Effects of MVT on solubility behaviour

Modification of side chains to tune polymer and copolymer properties is common practice when synthesising chain-growth polymers. TBRT allows this despite generating branched polymers that are analogous to step-growth polymerisations. Within conventional step-growth chemistries, the structure of the backbone is typically varied by copolymerisation. TBRT also allows this to be achieved by variation of MVT. To enable gross effects to be studied, BPADMA was selected as it is hydrophobic, aromatic, and rigid when compared to GDMA.

When comparing the homopolymers p(DDT-GDMA), p(*t*BuBzM-GDMA), and p(TG-GDMA), **1–3**, with the analogous BPADMA-derived homopolymers p(DDT-BPADMA), **10**, p(*t*BuBzM-BPADMA), **11**, and p(TG-BPADMA), **12**, a considerable contrast in solubility behaviour can be seen. Firstly, no appreciable water solubility is observed for these latter homopolymers with the aromatic MVT clearly dominating the low hydrophilicity of the materials, even in the presence of thioglycerol side chains, Fig. 2B. The same impact of BPADMA can be seen within the methanol solubility data with all of the homopolymers residing within the "poorly soluble" category. Notably, p(DDT-BPADMA), **10**, has appreciable solubility in hexane ([hexane] = 28.2 mg mL^{-1}) whilst p(*t*BuBzM-BPADMA), **11**, is considered "slightly soluble" under the criteria used in this study ([hexane] = 5.2 mg mL^{-1}). The interplay of hydrophilicity and hydrophobicity within p(TG-BPADMA), **12**, appears to impede hexane solubility, Fig. 2B.

A similar comparison can be made within the IBOMA-containing copolymers synthesised from each MVT. Firstly, the water solubility of the copolymers p([DDT-BPADMA]-*stat*-IBOMA), **13**, p([*t*BuBzM-BPADMA]-*stat*-IBOMA), **14**, and p([TG-BPADMA]-*stat*-IBOMA), **15**, all mirror the "poorly soluble" nature of the equivalent GDMA-derived copolymers (**7–9**). The presence of BPADMA residues within the branched copolymer backbones was seen to impact methanol solubility relative to GMDA-derived backbones. p([DDT-BPADMA]-*stat*-IBOMA), **13**, and p([*t*BuBzM-BPADMA]-*stat*-IBOMA), **14**, remained within the "slightly soluble" category but, most notably, p([TG-BPADMA]-*stat*-IBOMA), **15**, solubility fell from "highly soluble" (p([TG-GDMA]-*stat*-IBOMA), **9**, [methanol] = 84.7 mg mL^{-1}) to "slightly soluble" ([methanol] = 9.3 mg mL^{-1}) on the introduction of the aromatic backbone, Fig. 2C. This clearly mirrors the behaviour seen within the two homopolymer series where the comparison of p(TG-GDMA), **3**, and p(TG-BPADMA), **12**, showed a near identical impact on methanol solubility from the aromatic MVT.

Finally, the hexane solubility of the IBOMA-containing copolymers may be compared across the two MVTs. As seen for p([DDT-GDMA]-*stat*-IBOMA), **7**, p([DDT-BPADMA]-*stat*-IBOMA), **13**, showed the greatest solubility in hexane across the three telogen copolymers and was determined to be "highly soluble" within our categorisation. Interestingly, p([DDT-BPADMA]-*stat*-IBOMA), **13**, was not as soluble as p([DDT-GDMA]-*stat*-IBOMA), **7**, suggesting an effect from the MVT chemistry that is not immediately clear although a molecular weight effect cannot be ruled out; p([DDT-GDMA]-*stat*-IBOMA), **7**, is one of the two copolymer samples with M_w < 50 000 g mol^{-1}. p([*t*BuBzM-BPADMA]-*stat*-IBOMA), **13**, showed a significantly higher solubility ([hexane] = 17.6 mg mL^{-1}) than its GDMA copolymer analogue, also mirroring the comparative behaviour of the homopolymer series. Although p([TG-BPADMA]-*stat*-IBOMA), **15**, showed "poor solubility" in hexane, the negative impact of the 1-thioglycerol side group is considerable, overcoming the solvent interactions of the BPDMA and IBOMA residues within the copolymer.

Solubility behaviour of the GDMA-derived homopolymer and statistical copolymer series

Across the GDMA-derived TBRT homopolymers and statistical copolymers, GMA, MEMA, GlyMA and IBOMA were all used as mono-VTs and DDT, *t*BuBzM and TG were combined with all GDMA polymerisations. The solubility of all fifteen GDMA backbone polymers were studied in the seven solvents of interest, and the results were grouped for each telogen to present the impact of solvent and homo-/copolymer composition, and several clear trends are readily discernible, Fig. 3.

Appreciable solubility in water is only achievable when using TG as the telogen. This is not necessarily unexpected, and the inclusion of GMA, MEMA, and GlyMA within p([TG-GDMA]-*stat*-XXX) copolymers enhances the solubility over the "slightly soluble" homopolymer p(TG-GDMA), **3**. The positive impact of GlyMA on water solubility was not expected, with p([TG-GDMA]-*stat*-GlyMA), **19**, showing the highest water solubility of the GDMA-derived polymer series. Inclusion of IBOMA was able to overcome the water-polymer interactions to generate a water insoluble, but hydroxyl-functional copolymer.

The p(TG-GDMA) homopolymer and all p([TG-GDMA]-*stat*-XXX) copolymers were "highly soluble" in methanol, with GlyMA again showing considerable impact on the measured values (p([TG-GDMA]-*stat*-GlyMA), **21**, [methanol] = 115.1 mg mL^{-1}). Only GMA containing copolymers were measured as "highly soluble" in methanol when *t*BuBzM or DDT were used as telogen. It is notable that again, the inclusion of GlyMA enabled methanol solubility within the "soluble" range even when *t*BuBzM or DDT were present, suggesting a relatively strong interaction with methanol.

"High solubility" was observed in both acetone and THF for all DDT- and *t*BuBzM-containing homo- and copolymers derived from GDMA, however, only one copolymer within the TG-derived series showed comparable solubility in acetone (p([TG-GDMA]-*stat*-IBOMA), **9**; [acetone] = 86.8 mg mL^{-1}) and

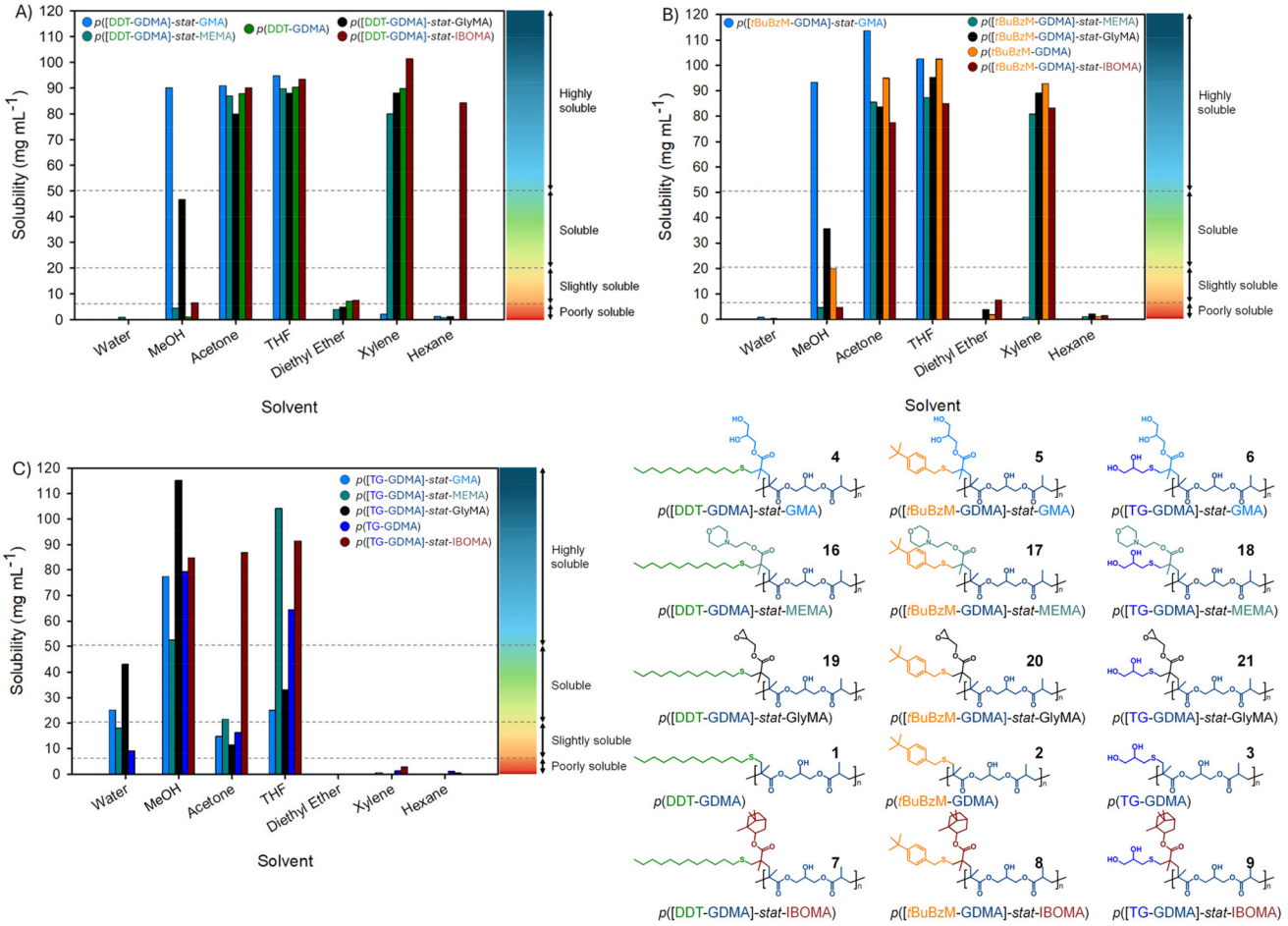

Fig. 3 Comparative solubilities in a range of solvents of GDMA-derived homopolymers and statistical copolymers synthesised using TBRT. (A) Materials synthesised using DDT as the telogen (**4**, **16**, **19**, **1**, **7**); (B) materials synthesised using *t*BuBzM as the telogen (**5**, **17**, **20**, **2**, **8**); (C) materials synthesised using TG as the telogen (**6**, **18**, **21**, **3**, **9**). Data shown as experimental values and compared against a scale ranging from poorly soluble through to highly soluble.

only three polymers, namely p([TG-GDMA]-*stat*-MEMA) **18**, p(TG-GDMA) **3**, and p([TG-GDMA]-*stat*-IBOMA) could be categorised as "highly soluble" in THF.

No polymers with a GDMA-derived backbone were considered "soluble" or "highly soluble" in diethyl ether, although the highest number of structures with measurable solubility were seen from DDT-containing materials. The highest solubilities in diethyl ether were recorded for the IBOMA copolymers p([DDT-GDMA]-*stat*-IBOMA), **7**, and p([*t*BuBzM-GDMA]-*stat*-IBOMA), **8**, with values < 8.0 mg mL^{-1} but categorised as "slightly soluble" when applying our scale.

TG-containing homo- and copolymers within this series were essentially insoluble in xylene and hexane; however, "high solubility" in xylene was seen across both DDT- and *t*BuBzM-derived samples apart from those containing GMA, where the measured values were clearly within the "poorly soluble" category. The use of *t*BuBzM as telogen was unable to generate appreciable solubility across any composition studied, and only p([DDT-GDMA]-*stat*-IBOMA), **7**, showed hexane solubility, as discussed above.

Solubility behaviour of the BPADMA-derived homopolymer and statistical copolymer series

A similar telogen grouping was applied to the BPADMA-derived series of fifteen homo- and statistical copolymers, Fig. 4, leading to identification of similar trends to those seen within the GDMA-derived series and some BPADMA specific behaviour.

"Poor solubility" in water was seen for all materials containing BPDMA residues within the polyester backbone, apart from two of the TG-derived copolymers. Both p([TG-BPADMA]-*stat*-MEMA), **27**, p([TG-BPADMA]-*stat*-GlyMA), **30**, showed comparable solubility in water to their GDMA-derived counterparts, with GlyMA inclusion again shown to produce the most water-soluble polymer (p([TG-BPADMA]-*stat*-GlyMA), [water] = 38.7 mg mL^{-1}).

Methanol solubility of BPADMA-derived polymers containing DDT and *t*BuBzM telogen residues was restricted to the

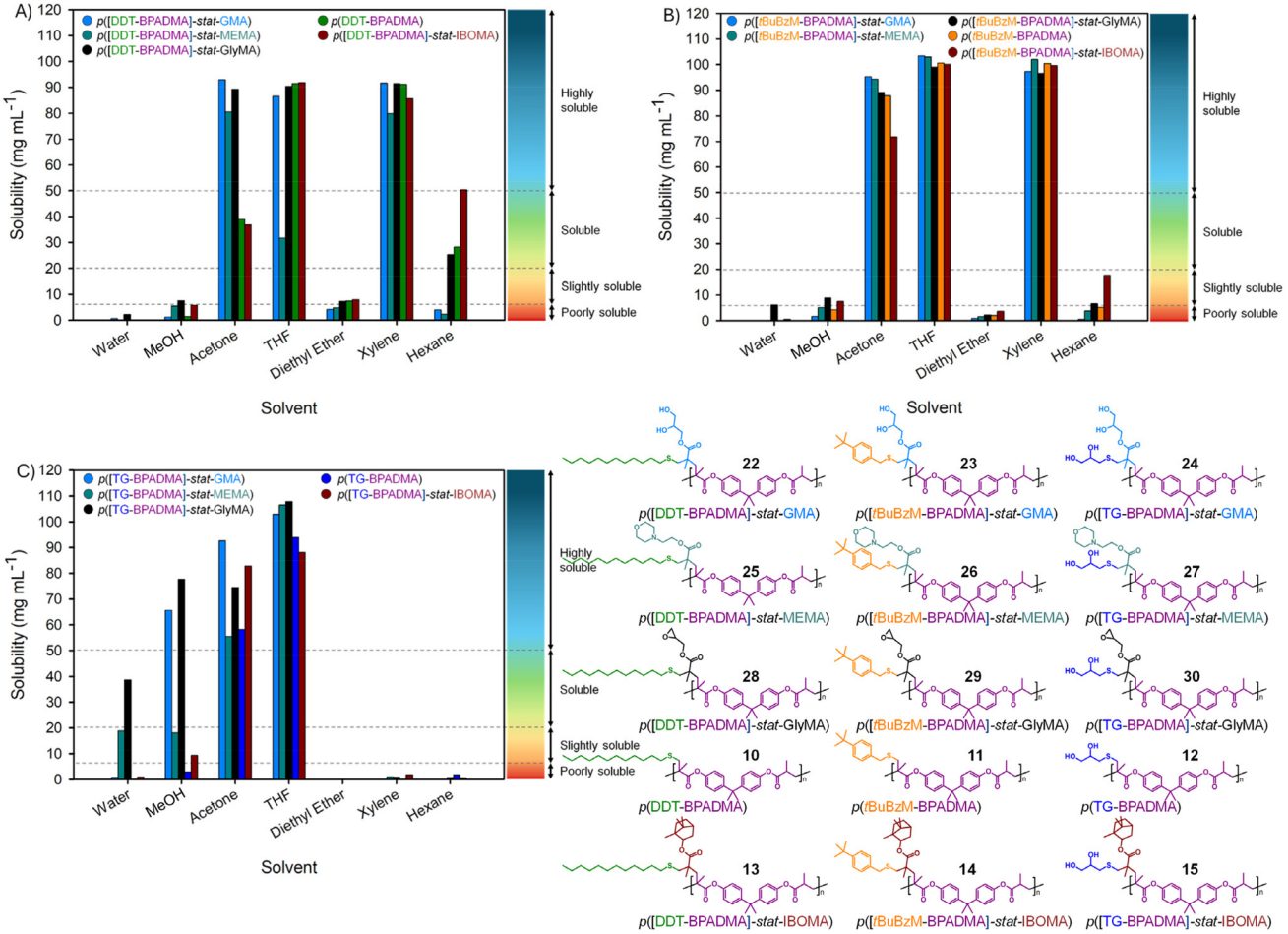

Fig. 4 Comparative solubilities in a range of solvents of BPADMA-derived homopolymers and statistical copolymers synthesised using TBRT. (A) Materials synthesised using DDT as the telogen (**22**, **25**, **28**, **10**, **13**); (B) materials synthesised using *t*BuBzM as the telogen (**23**, **26**, **29**, **11**, **14**); (C) materials synthesised using TG as the telogen (**24**, **27**, **30**, **12**, **15**). Data shown as experimental values and compared against a scale ranging from poorly soluble through to highly soluble.

"poorly soluble" or "slightly soluble" categories. The solubility of TG-derived polymers in this series was also impacted by the aromatic backbone, although p([TG-BPADMA]-*stat*-GMA), **24**, and p([TG-BPADMA]-*stat*-GlyMA), **30**, were observed to be "highly soluble" and, again, the presence of GlyMA aided polymer solubilisation significantly within this solvent.

All branched polymers with BPADMA-derived backbones showed excellent solubility in acetone and THF with only three DDT-containing polymers falling outside of the "highly soluble" category. p(DDT-BPADMA) (**10**, [acetone] = 38.9 mg mL^{-1}) and p([DDT-BPADMA]-*stat*-IBOMA), (**13**, [acetone] = 36.8 mg mL^{-1}) both appear in the "soluble" category in acetone, whilst p([DDT-BPADMA]-*stat*-MEMA), (**25**, [THF] = 31.7 mg mL^{-1}) was determined to be "soluble" in THF.

As seen with the GDMA-derived series, the BPADMA backbone polymers formed using TG had no appreciable solubility in diethyl ether, xylene, or hexane. All polymers formed using DDT or *t*BuBzM also showed limited solubility in diethyl ether, although all five of the DDT-containing materials consistently showed higher solubilities in this solvent than those utilising *t*BuBzM or TG. When DDT and *t*BuBzM was present as side chains the materials were "highly soluble" in xylene, mirroring the same observation when using the GDMA MVT.

BPADMA residues clearly lead to positive polymer-hexane interactions, with six polymers being classified as "slightly soluble" or better compared to just one within the GDMA-derived series: p([DDT-BPADMA]-*stat*-GlyMA), (**28** [hexane] = 25.3 mg mL^{-1}); p(DDT-BPADMA), (**10** [hexane] = 28.2 mg mL^{-1}); p([DDT-BPADMA]- *stat*-IBOMA), (**25** [hexane] = 50.3 mg mL^{-1}); p([*t*BuBzM-BPADMA]-*stat*-GlyMA), (**29** [hexane] = 6.6 mg mL^{-1}); p([*t*BuBzM]-BPADMA), (**11** [hexane] = 5.2 mg mL^{-1}); and p([*t*BuBzM-BPADMA]-*stat*-IBOMA), (**15** [hexane] = 17.6 mg mL^{-1}).

Model prediction of TBRT polymer solubility trends

As mentioned earlier, predicting the solubility of unknown solids is difficult, even for novel small molecules.[41] Several

computational models have emerged that require specific physical data to be collected prior to prediction,[42] and several are limited in their scope of solvents that may be modelled; water solubility has, for obvious reasons, dominated the focus of such models and deep neural networks have been trained using existing experimental data.[43]

Recently, an approach has been reported for solid solubility prediction that does not rely on collecting experimental data for unknown compounds prior to modelling across approximately 100 solvents. The sole input parameters are the SMILES (Simplified Molecular Input Line Entry System) strings for the solute and chosen solvent, and the required temperature. The open access online predictor utilises a deep neural network that was trained using considerable databases, one of which contains quantum chemical data (CombiSolv-QM) and another with a large experimental dataset (CombiSolv-Exp).[44] Through the combination of machine learning and a series of thermodynamic calculations, solid solubility of neutral compounds in neutral solvents is predicted as $c\log S$, in addition to a number of other predicted parameters including solvation enthalpy, solvation entropy and heat capacity.[45]

To investigate the potential for such models to provide guidance on solubilities of TBRT polymers, the thirty branched homo- and statistical copolymers synthesised here were reduced to their nominal repeat units, Fig. 3 & 4, and the corresponding SMILES strings were used as the sole input parameter for the polymers (Fig. S5 & 6). Each of the seven solvents were also used as SMILES inputs and the selected temperature for the predictions was consistent at 298 K; the model is hosted on the Reaction Mechanism Generator (RMG) website.[46]

When comparing the experimental solubility data for the GDMA-derived homopolymers, Fig. 5A, to the calculated $\log S$ values from the model, it is clear that the predicted values are not accurate, however, within a single solvent the model is generally very good at predicting the directionality of solubility across the varying telogen residues.

For example, the model predicts that p(DDT-GDMA), **1**, has a low solubility in methanol when compared to p(*t*BuBzM-GDMA), **2**, which is predicted to be less soluble than p(TG-GDMA), **3**, and this is borne out within the experimental values. This same directional correlation is seen within the predictions of solubilities in water, acetone, THF, diethyl ether, and xylene. Hexane solubility does not correlate well for these homopolymers. Within a single homopolymer, the correlation across solvents is also relatively accurate from a directional perspective. As an example, p(TG-GDMA), **3**, is predicted to be less soluble in water than methanol, with a subsequent decrease in solubility in acetone, and THF, with very low solubility in diethyl ether xylene and hexane; this is indeed in good correlation with the experimental data and the same good correlations are also seen for p(DDT-GDMA), **1**, and p(*t*BuBzM-GDMA), **2**.

Considering the correlation of predicted solubility behaviour and experimental data for BPDMA-derived homopolymers, Fig. 5B, the ordering within each solvent across the different telogen-containing homopolymers is less correlated, but the model does well in showing the variability in expected solubility for a single homopolymer across the seven solvents studied, including predicting solubility in hexane and the relative order of solubilities in this solvent across the three homopolymers. "Poorly soluble" and insoluble samples were generally well represented by predicted negative values of $c\log S$.

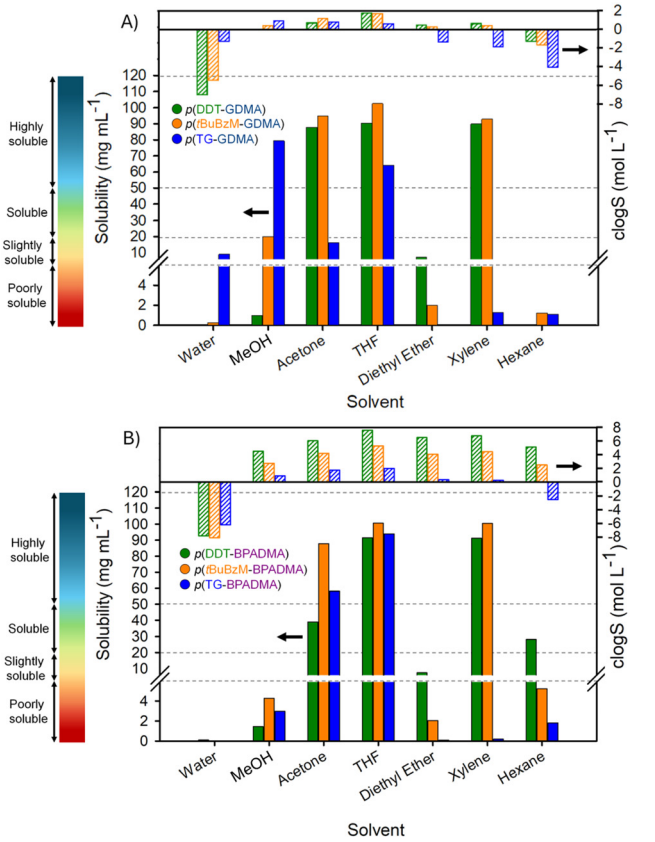

Fig. 5 Comparison of experimental solubilities and predicted $c\log S$ values for a range of homopolymers synthesised by TBRT across a selection of solvents. (A) GDMA-derived homopolymers and (B) BPADMA-derived homopolymers.

As an example of the simulation of solubility for statistical copolymers, Fig. 6 shows GDMA and BPADMA backbone materials with GlyMA as the mono-VT across all three telogens. The trends in the relative behaviour of p([DDT-GDMA]-*stat*-GlyMA), **19**, and p([*t*BuBzM-GDMA]-*stat*-GlyMA), **20**, are reasonably consistent between the modelled solubility and the experimental outcomes, Fig. 6A. Again, the exact $c\log S$ values are not expected to be accurate, but the predicted insolubility in water and increasing solubility of both polymers in methanol, acetone and THF follow the experimental trend, as does the relative decrease in solubility for both statistical copolymers in diethyl ether, increased solubility in xylene and subsequent "poor solubility" in hexane. It is clear that the solubility in diethyl ether is predicted to be nearly equivalent to that in methanol and this is clearly not borne out by the experimental measurements. The model appears to struggle to predict trends for p([TG-GDMA]-*stat*-GlyMA), **21**, in the higher polarity solvents, especially water, but correctly highlights the observed lack of solubility in diethyl ether, xylene and hexane.

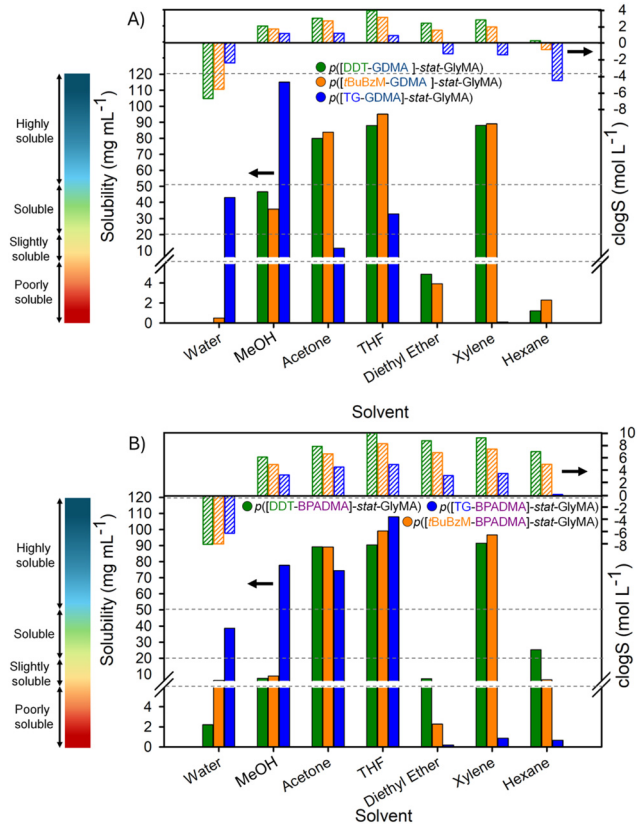

Fig. 6 Comparison of experimental solubilities and predicted *c* log *S* values for a range of GlyMA-containing statistical copolymers synthesised by TBRT across a selection of solvents. (A) GDMA-derived statistical copolymers and (B) BPADMA-derived statistical copolymers.

The equivalent statistical copolymers derived from BPADMA have solubility trends that also align reasonably well with prediction, Fig. 6B. Solubility in water is predicted as being low for all three statistical copolymers, despite experimental values showing acceptable solubility for p([TG-BPADMA]-*stat*-GlyMA), **30**. Diethyl ether solubility again appears to be difficult to predict for these branched polyesters, and the model appears to incorrectly indicate the potential for p([TG-BPADMA]-*stat*-GlyMA) in low polarity solvents.

On a final note, the repeated examples of GlyMA incorporation improving experimental methanol and water solubilities over highly hydrophilic side chains such as GMA were unexpected and not readily rationalised. The models employed here also predict *c* log *S* values for GlyMA containing polymers being very similar to those containing GMA in these solvents and, in some cases, higher solubilities where GlyMA is employed (*e.g.* methanol solubility: p([DDT-BPADMA]-*stat*-GlyMA) > p([DDT-BPADMA]-*stat*-GMA)).

Conclusions

The understanding of TBRT is evolving and as the branched polymers and copolymers that may be generated by this technique are very new, it is important to study their physical and chemical behaviour. It is perhaps not entirely surprising that variations in the structure of telogen, MVT and mono-VT can have significant impact on the solubility of these materials. Within the homopolymers shown here, this is not dissimilar to the impact of varying a side chain in a methacrylate series such as p(lauryl methacrylate), p(benzyl methacrylate), and p(glycerol methacrylate). That said, it is not possible in such a series to modify the backbone from the C–C methacrylate structure, but TBRT allows this through the change in MVT. The incorporation of extra side chains through the inclusion of mono-VTs is also different to conventional polymers, although can be viewed as analogous to statistical copolymerisation of varying vinyl monomers.

The solubility trends described herein do show a simple view of solvent diversity (polarity, dipole moment, dielectric constant, or eluotropic strength) is not able to directly gauge even the directional variation within the most simple TBRT homopolymers. MVT backbone chemistry can clearly predominate within the solubility behaviour of homopolymers and statistical copolymers alike. Mono-VT may be utilised to balance or negate the impact of backbone chemistry and introduce strong solvent interactions that modify polymer behaviour in surprising ways. Here we have attempted to utilise a relatively new machine learning-derived solubility prediction that has indeed been shown to provide insight into what may be expected to be seen in these new materials. This has solely utilised the repeat unit chemistry within each sample with “slightly” and “poorly soluble” being relatively well indicated by the model. The degree of predictability was reasonable, especially given the complexity of rationalising polymer solubility using existing complex mathematical models. As these models continue to improve, the accuracy, and potentially the actual solubility values, would be expected to become more closely associated with experimental measurement. The ability to manipulate TBRT polymer and copolymer solubility is important for future applications.

Author contributions

BL contributed to conceptualisation of the study and conducted the bulk of the experimental investigation, data analysis and production of the draft manuscript. SF, SM, SW and SRC contributed to supervision and methodology. PC contributed to methodologies, supervision and experimental investigation. OBP-L and ABD contributed to supervision, methodology, data curation and editing of the original and final drafts. SLB, PHF and MD contributed to funding, methodologies, supervision, review of final drafts and project administration. SPR was responsible for funding acquisition, conceptualisation of the original research programme, methodology, validation, visualisation, supervision, data analysis, project administration and manuscript drafting, review and editing.

Conflicts of interest

SRC, SW, PC and SPR are co-inventors on patents that protect the TBRT chemistry. No other co-authors have any competing interests.

Data availability

Data generated during this study supporting its findings are available within the manuscript and the supplementary information (SI). Supplementary information: materials, full experimental details and characterisation. See DOI: https://doi.org/10.1039/d6py00352d.

All data are available from the corresponding author upon reasonable request.

Acknowledgements

The Engineering & Physical Sciences Research Council (EPSRC) are grateful acknowledged for funding through grants EP/R010544/1 and EP/X010864/1. BL and MD are grateful for studentship funding from Scott Bader. SM is grateful for studentship funding from EPSRC and Unilever. OBPL is grateful for studentship funding from EPSRC and the University of Liverpool. The authors would like to thank the Materials Innovation Factory (University of Liverpool) for access to analytical facilities.

References

1 N. Corrigan, K. Jung, G. Moad, C. J. Hawker, K. Matyjaszewski and C. Boyer, *Prog. Polym. Sci.*, 2020, **111**, 101311.
2 A. Hirao, R. Goseki and T. Ishizone, *Macromolecules*, 2014, **47**, 1883–1905.
3 T. Alhilfi, P. Chambon and S. P. Rannard, *J. Polym. Sci., Part A:Polym. Chem.*, 2020, **58**, 1426–1438.
4 J. Ethier, E. R. Antoniuk and B. Brettmann, *Soft Matter*, 2024, **20**, 5652–5669.
5 D. J. Fowles, B. J. Connaughton, J. W. Carter, J. B. O. Mitchell and D. S. Palmer, *Chem. Rev.*, 2025, **125**, 7057–7098.
6 R. Spann and D. Boucher, *J. Polym. Sci.*, 2023, **61**, 503–514.
7 S. Venkatram, C. Kim, A. Chandrasekaran and R. Ramprasad, *J. Chem. Inf. Model.*, 2019, **59**, 4188–4194.
8 P. Zhou, J. Yu, K. L. Sánchez-Rivera, G. W. Huber and R. C. Van Lehn, *Green Chem.*, 2023, **25**, 4402–4414.
9 M. Denayer, J. Vekeman, F. Tielens and F. De Proft, *Phys. Chem. Chem. Phys.*, 2021, **23**, 25374–25387.
10 M. Amrihesari, J. Kern, H. Present, S. Moreno Briceno, R. Ramprasad and B. Brettmann, *J. Phys. Chem. B*, 2024, **128**, 12786–12797.
11 H. W. Milliman, D. Boris and D. A. Schiraldi, *Macromolecules*, 2012, **45**, 1931–1936.
12 L. Smith, H. A. Karimi-Varzaneh, S. Finger, G. Giunta, A. Troisi and P. Carbone, *Macromolecules*, 2024, **57**, 4637–4647.
13 S. Mohammed, L. Budach, M. Feuerpfeil, N. Ihde, A. Nathansen, N. Noack, H. Patzlaff, F. Naumann and H. Harmouch, *Inf. Syst.*, 2025, **132**, 102549.
14 M. Amrihesari, A. Murry and B. Brettmann, *Polymer*, 2023, **278**, 125983.
15 Y. Aoki, S. Wu, T. Tsurimoto, Y. Hayashi, S. Minami, O. Tadamichi, K. Shiratori and R. Yoshida, *Macromolecules*, 2023, **56**, 5446–5456.
16 S. R. Cassin, P. Chambon and S. P. Rannard, *Polym. Chem.*, 2020, **11**, 7637–7649.
17 S. R. Cassin, S. Flynn, P. Chambon and S. P. Rannard, *Polym. Chem.*, 2022, **13**, 2295–2306.
18 S. Mckeating, O. B. Penrhyn-Lowe, S. Flynn, S. R. Cassin, S. Lomas, C. Fidge, P. Price, S. Wright, P. Chambon and S. P. Rannard, *Commun. Chem.*, 2024, **7**, 197.
19 A. B. Dwyer, W. M. Sandy, F. Y. Hern, O. B. Penrhyn-Lowe, S. McKeating, S. Flynn, S. Wright, S. Pate, P. Chambon and S. P. Rannard, *Chem. Commun.*, 2024, **60**, 10116–10119.
20 O. B. Penrhyn-Lowe, S. Flynn, S. R. Cassin, S. Mckeating, S. Lomas, S. Wright, P. Chambon and S. P. Rannard, *Polym. Chem.*, 2021, **12**, 6472–6483.
21 S. Flynn, O. B. Penrhyn-Lowe, S. Mckeating, S. Wright, S. Lomas, S. R. Cassin, P. Chambon and S. P. Rannard, *RSC Adv.*, 2022, **12**, 31424–31431.
22 B. Boutevin, *J. Polym. Sci., Part A:Polym. Chem.*, 2000, **38**, 3235–3243.
23 S. Mckeating, C. Smith, O. B. Penrhyn-Lowe, S. Flynn, S. Wright, P. Chambon, A. Dwyer and S. Rannard, *Polym. Chem.*, 2025, **16**, 1131–1138.
24 S. Flynn, B. Linthwaite, O. B. Penrhyn-Lowe, S. Mckeating, S. Wright, S. R. Cassin, P. Chambon and S. P. Rannard, *Polym. Chem.*, 2023, **14**, 5102–5511.
25 D. Avci and L. J. Mathias, *Polymer*, 2004, **45**, 1763–1769.
26 S. R. Cassin, S. Wright, S. Mckeating, O. B. Penrhyn-Lowe, S. Flynn, S. Lomas, P. Chambon and S. P. Rannard, *Polym. Chem.*, 2023, **14**, 1905–1914.
27 C. Smith, O. B. Penrhyn-Lowe, S. Mckeating, S. Wright, A. B. Dwyer and S. P. Rannard, *Polym. Chem.*, 2025, **16**, 1486–1492.
28 S. Cassin, S. Flynn, P. Chambon and S. P. Rannard, *RSC Adv.*, 2021, **11**, 24374–24380.
29 L. Xochicale-Santana, C. C. Vidyasagar, B. M. Muñoz-Flores and V. M. Jiménez Pérez, in *Handbook of Greener Synthesis of Nanomaterials and Compounds: Volume 1: Fundamental Principles and Methods*, ed. B. Kharisov and O. Kharissova, Elsevier, Amsterdam, 2021, ch. 15, pp. 491–542.
30 S. Spange, N. Weiß, C. H. Schmidt and K. Schreiter, *Chem. Methods*, 2021, **1**, 42–60.
31 A. M. Striegel, *TrAC, Trends Anal. Chem.*, 2020, **130**, 115990.
32 J. Tejas, B. Patel and L. D. Patel, *Int. Res. J. Pharm.*, 2012, **3**, 106–113.
33 K. T. Savjani, A. K. Gajjar and J. K. Savjani, *ISRN Pharm.*, 2012, 195727.

34 C. Ramkissoon-Ganorkar, L. Feng, M. Baudys and S. W. Kim, *J. Biomater. Sci., Polym. Ed.*, 1999, **10**, 1149–1161.
35 J. S. Papanu, D. S. Soane, A. T. Bell and D. W. Hess, *J. Appl. Polym. Sci.*, 1989, **38**, 859–885.
36 T. Zhu and T. Van Voorhis, *J. Phys. Chem. Lett.*, 2021, **12**, 6–12.
37 C. Schubert, C. Osterwinter, C. Tonhauser, M. Schömer, D. Wilms, H. Frey and C. Friedrich, *Macromolecules*, 2016, **49**(22), 8722–8737.
38 E. Malmström, M. Johansson and A. Hult, *Macromolecules*, 1995, **28**, 1698–1703.
39 M. R. Saeb, Y. Mohammadi, H. Rastin, T. S. Kermaniyan and A. Penlidis, *Macromol. Theory Simul.*, 2017, **26**, 1700041.
40 Y. Zhu, J. Ziebarth, T. Macko and Y. Wang, *Macromolecules*, 2010, **43**, 5888–5895.
41 M. Kuentz and C. A. S. Bergström, *Pharm. Sci.*, 2021, **110**, 22–34.
42 H. Renon, *Fluid Phase Equilib.*, 1985, **24**, 87–114.
43 A. Lusci, G. Pollastri and P. Baldi, *J. Chem. Inf. Model.*, 2013, **53**, 1563–1575.
44 F. H. Vermeire and W. H. Green, *Chem. Eng. J.*, 2021, **418**, 129307.
45 F. H. Vermeire, Y. Chung and W. H. Green, *J. Am. Chem. Soc.*, 2022, **144**, 10785–10797.
46 RMG-database (accessed 9th April 2026)https://rmg.mit.edu/database/solvation/searchSolubility/.